Science Advances
AAAS

advances.sciencemag.org/cgi/content/full/6/21/eaay7735/DC1

Supplementary Materials for

Self-healing microcapsules synergetically modulate immunization microenvironments for potent cancer vaccination

Xiaobo Xi, Tong Ye, Shuang Wang, Xiangming Na, Jianghua Wang, Shuang Qing, Xiaoyong Gao, Changlong Wang, Feng Li, Wei Wei*, Guanghui Ma*

*Corresponding author. Email: weiwei@ipe.ac.cn (W.W.); ghma@ipe.ac.cn (G.M.)

Published 22 May 2020, *Sci. Adv.* **6**, eaay7735 (2020)
DOI: 10.1126/sciadv.aay7735

This PDF file includes:

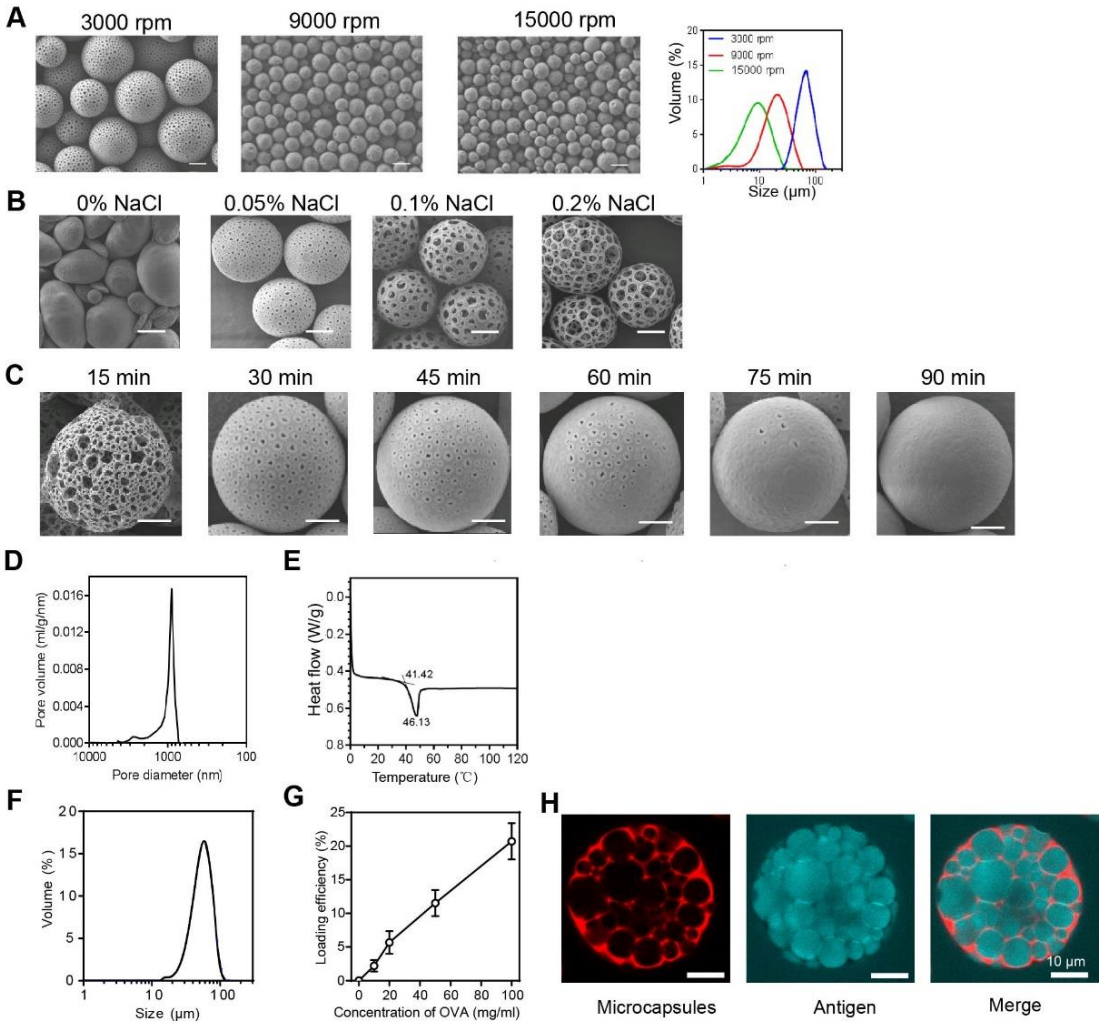

fig. S1. Fabrication and characterizations of gigaporous microspheres and resulted microcapsule formulation

A) **Morphology and size distribution of gigaporous microspheres at different homogenizer speeds.** With the increase of homogenizer speed**,** the surface pores closed and the size of microspheres decreased. Considering the suitable size for *in situ* depot and gigaporous structure for antigen loading, 3000 rpm was regarded as the optimum. Scale bar: 20 μm.

B) **Effect of NaCl concentration on microsphere morphology.** The addition of NaCl in the inner water phase resulted in the surface pore, and the pore size increase with the NaCl concentration. Considering the suitable pore size for healing, 0.05% was regarded as the optimum. Scale bar: 10 μm.

C) **Effect of evolution time on surface pores.** The number and size of pores on the surface decreased with the increased evolution time. To facilitate the antigen loading and subsequent healing, 30 min was regarded as the optimum. Scale bar: 10 μm.

D) **Pore size distribution of gigaporous microspheres.** The porosity rate was detected to be ~82%, and the pore diameter ranged from 900 nm to 5 μm.

E) **Healing temperature of gigaporous microspheres.** As differential scanning calorimetry (DSC) curve of microspheres showed the glass transition temperature

(Tg) was 41.42℃, self-healing microcapsules could be prepared at~40℃ within 2 hours.

F) **Size distribution of microcapsules after the healing process.** The mean size of microcapsules was detected around 50 μm.

G) **OVA loading efficiency (LE) within self-healing microcapsules.** The LE increased as the initial antigen concentration increased, which ensured that loading capacity could be controlled by modulating initial antigen concentration. (n=3).

H) **Observation of antigen encapsulation within self-healing microcapsules.** OVA (blue) clearly filled the cavities of microcapsules (red), indicating that antigen efficiently diffused into the microcapsules through the interconnected porous structure. Scale bar: 10 μm.

The bars in G represented means±s.d..

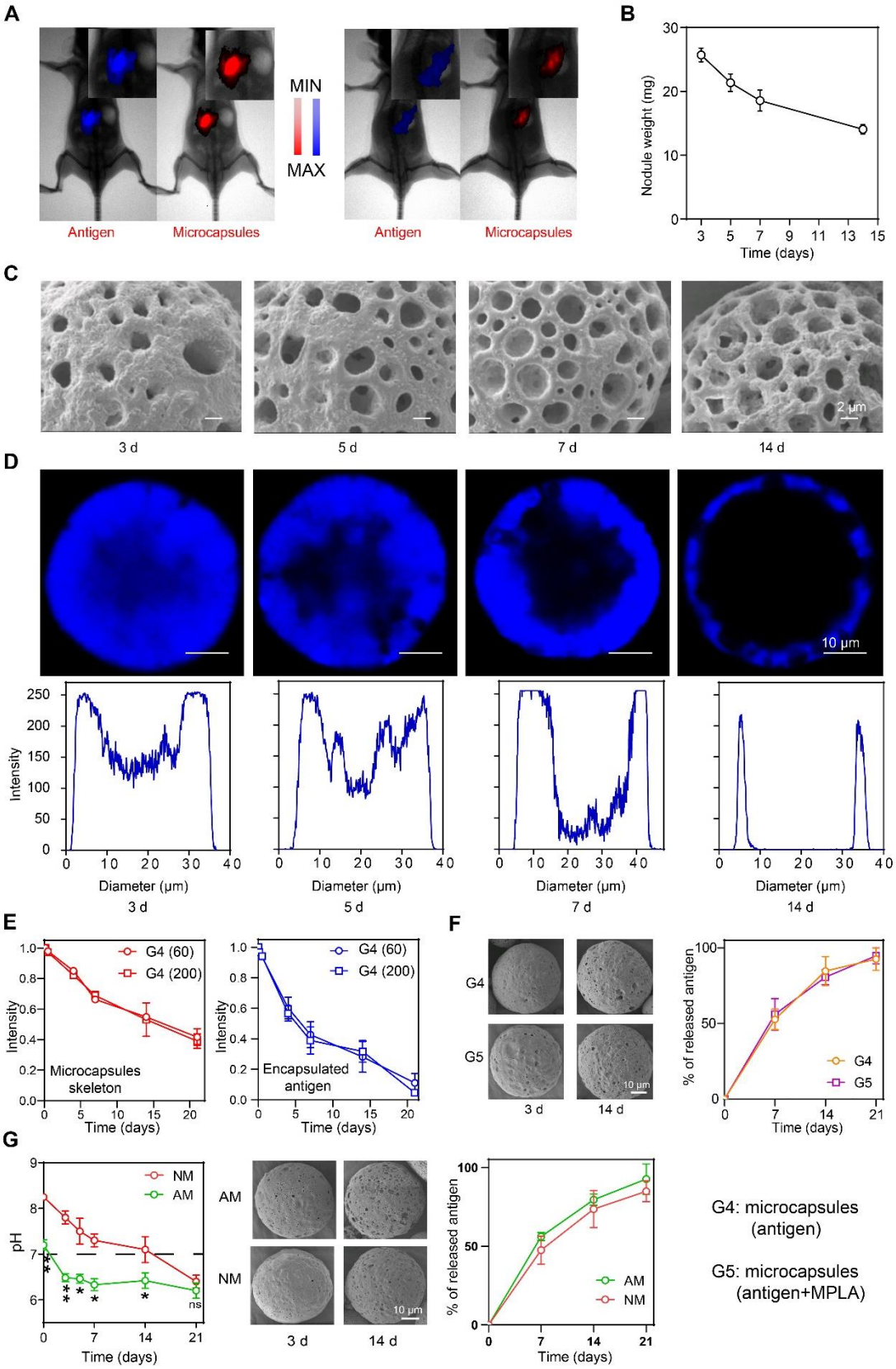
A
MIN
MAX
Antigen
Microcapsules
Antigen
Microcapsules
B
Nodule weight (mg)
Time (days)
C
2 μm
3 d
5 d
7 d
14 d
D
10 μm
Intensity
Diameter (μm)
3 d
5 d
7 d
14 d
E
G4 (60)
G4 (200)
Microcapsules skeleton
Encapsulated antigen
Intensity
Time (days)
F
G4
G5
10 μm
3 d
14 d
% of released antigen
Time (days)
G
NM
AM
pH
Time (days)
AM
NM
10 μm
3 d
14 d
% of released antigen
Time (days)
G4: microcapsules (antigen)
G5: microcapsules (antigen+MPLA)

fig. S2. Microcapsule degradation and antigen release profile.

A) **Comparison of antigen depot ability *in vivo* between self-healing microcapsules (left image) and gigaporous microspheres (right image) on day 3.** Antigen (blue) was more co-localized with microcapsules (red) than with microspheres (red), indicating the antigen depot by the microcapsules.

B) **Weight change of subcutaneous nodule.** The weight of *in situ* subcutaneous nodules decreased gradually after vaccination, indicating the biodegradability of formulation *in vivo*. (n=3).

C) **Morphology of microcapsules extracted from the vaccination site at different time points.** The skeleton was gradually eroded by hydrolysis, which paved the way for the sustained release of antigen at the vaccination site. Scale bar: 2 μm.

D) **OVA-Cy5 distribution in microcapsules extracted from the vaccination site at different time points.** The signal gradually disappeared from inside to outside. Such a phenomenon suggested that the exterior antigen had released ahead, which was followed by the outward migration of interior antigen. Scale bar: 10 μm.

E) **Influence of antigen does on the microcapsule degradation and antigen release *in vivo*.** G4 (60 μg): microcapsules loading with 60 μg antigen; G4 (200 μg): microcapsules loading with 200 μg antigen. The data were obtained by *in vivo* imaging of fluorescence signal sourced from labeled microcapsule and antigen. Similar antigen release kinetic was observed due to unchanged degradation behavior. (n=3).

F) **Influence of MPLA addition on the microcapsule degradation and antigen release *in vitro*.** G4: microcapsules loading with 200 μg antigen; G5: microcapsules loading with 200 μg antigen and 3 μg MPLA. Actually, low dose of MPLA scarcely interfered the degradation of microcapsules, which explained little difference on the antigen release kinetics. (n=3).

G) **Left panel: pH value quantification inside AM and NM microcapsules *in vivo*.** At the beginning, the pH value of NM microcapsules was slightly alkaline (pH=8.2). Over time, the pH value was gradually inclined to be neutral. In comparison with the acidic pH (~6.5) from day 3 for AM microcapsules, the pH value inside NM microcapsules still maintained above 7.0 at day 14. With further degradation of microcapsule, the excess acidic components reverse the pH value to ~6.5 at day 21. Therefore, the acidification of NM microcapsules largely lagged behind that of AM microcapsules, which extended the time window for our comparative investigation of the acidic and neutral microenvironments on subsequent APCs recruitment, antigen uptake, cross-presentation, and activation. (n=3). **Middle panel: SEM images of AM and NM microcapsules *in vitro***. AM and NM microcapsules were separately incubated in the cell medium (with addition of 0.02% NaN_3) at 37 ℃ and sampled at day 3 and day 14. As the acidic environment is favorable for PLA hydrolysis, we observed slightly suppressed microcapsule degradation by the addition of $NaHCO_3$. **Right panel: Comparison of antigen release profile between NM and AM microcapsules *in vitro*.** The samples at day 0, 7, 14, 21 were determined by Micro BCA protein assay kit. Taking the day 21 for an example, the accumulated OVA release in NM group

was only ~8% lower than that of AM group, indicating a feeble role of $NaHCO_3$ addition on the antigen release. (n=3).
The bars in B, E, F and G represented means±s.d..

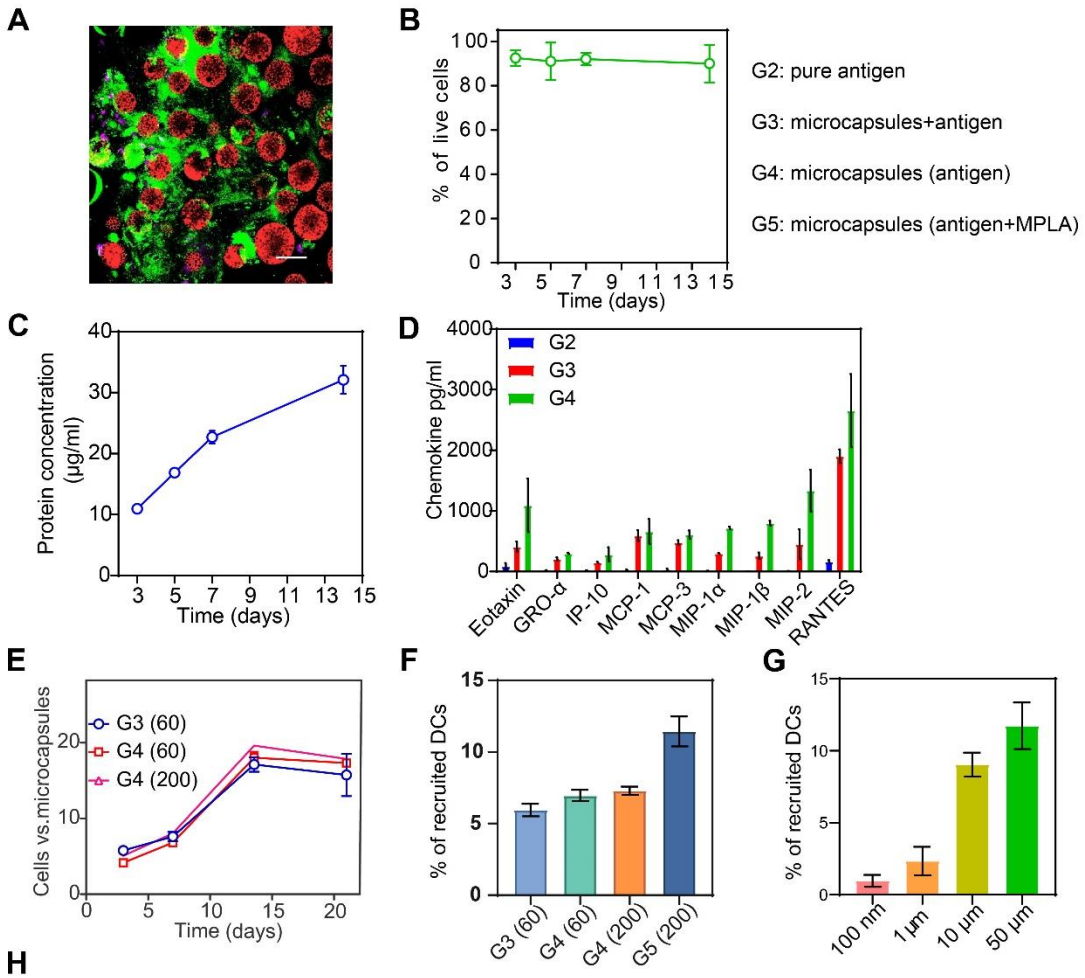

H

Chemokine	Full name	Receptor	main recruitment function
Eotaxin	Eotaxin	CCR3	Eosinophil and basophil migration
GRO-α	Growth-regulated oncogene-alpha	CXCR2	Neutrophil trafficking
IP-10	IFN-gamma-Inducible protein 10	CXCR3	CD8 T, NK trafficking
MCP-1,	Monocyte Chemoattractant Protein-1	CCR2	Monocyte trafficking; APCs recruitment
MCP-3	Monocyte Chemoattractant Protein-3	CCR2, CCR3	Monocyte mobilization; Regulation of macrophage
MIP-1α	Macrophage inflammatory protein-1 alpha	CCR1, CCR5	NK cell migration; APCs recruitment
MIP-1β	Macrophage inflammatory protein-1 beta	CCR5	NK cell migration; APCs recruitment
MIP-2	Macrophage Inflammatory Protein 2	CXCR2	Neutrophil chemotaxis and degranulation
RANTES	Regulated on Activation, Normal T cell Expressed and Secreted	CCR1, CCR3, CCR5	Eosinophil and basophil migration

fig. S3. Complementary investigations on APCs recruitment.

A) **Viability of recruited cells *in situ***. Green: live cells; magenta: dead cells; red: microcapsules. Most of recruited cells were alive, indicating the good biocompatibility of microcapsule. Scale bar: 50 μm.

B) **Viability of recruited cells at different time points.** More than 90% recruited cells were clearly alive, showing that microcapsules created a friendly microenvironment persistently *in situ*. (n=3).

C) **Protein concentration of local tissues at different time points.** The gradually increase protein concentration of local tissues indicated the persistent ability of cell recruitment by microcapsules. (n=3).

D) **Local secretion of chemokines.** Compared with mixed antigen group, the secretion levels of multiple chemokines in the encapsulated antigen group were elevated. (n=3).

E) **The ratio of recruited cells number to microcapsules number at different time points.** The recruitment of cell peaked at day 14, in accordance with Fig. 2B. Meanwhile, the data of different groups at the same time point showed no significant difference, indicating the neglectable influence of antigen release profile. (n=3).

F) **Analysis of DCs recruitment by flow cytometry.** G3 (60), antigen (60 μg) mixed with microcapsules; G4 (60), antigen (60 μg)encapsulated in healed microcapsules; G4 (200), antigen (200 μg)encapsulated in healed microcapsules; G5 (200): antigen (200 μg) encapsulated in healed microcapsules with 3 μg MPLA. No significant difference was observed among G3 (60), G4 (60) and G4 (200) groups, again indicating the neglectable influence of antigen release profile on DCs recruitment. However, G5 (200) group showed a higher value, demonstrating the important role of MPLA addition even with a low dose. (n=3).

G) **Effect of microcapsule size on DCs recruitment *in vivo*.** We subcutaneous injected the same dose of PLA-based particles with different size (100 nm, 1 μm, 10 μm and 50 μm) and collected the injection site tissue at day 14 for subsequent detection of recruited DCs. The microcapsules with an average size of 50 μm succeeded in the DCs recruitment, which might be attributed to the inflammatory response to the depot of exogenous material at the vaccination site. Such a capacity was gradually compromised with the decrease of particle size. Of note, very few DCs were detected at the nanoparticles-vaccination site, due to their rapid spread to other tissues/organs (e.g. lymph node). (n=3).

H) **Information of chemokines tested in the manuscript.** Among them, MIP-1α, MIP-1β, MIP-2 and MCP-1, MCP-3 show direct function for recruitment of macrophages and dendritic cells, which have been identified as professional APCs. Meanwhile, high secretion of Eotaxin and RANTES should also be considered. These two chemokines are well known to migrate eosinophil and basophil, which can also secreted chemokines (such as MIP-1) for APCs recruitment in an indirect manner. For GRO and IP-10, the low secretion and incapacity of APCs recruitment thus excludes their critical role.

The bars in B-G represented means±s.d..

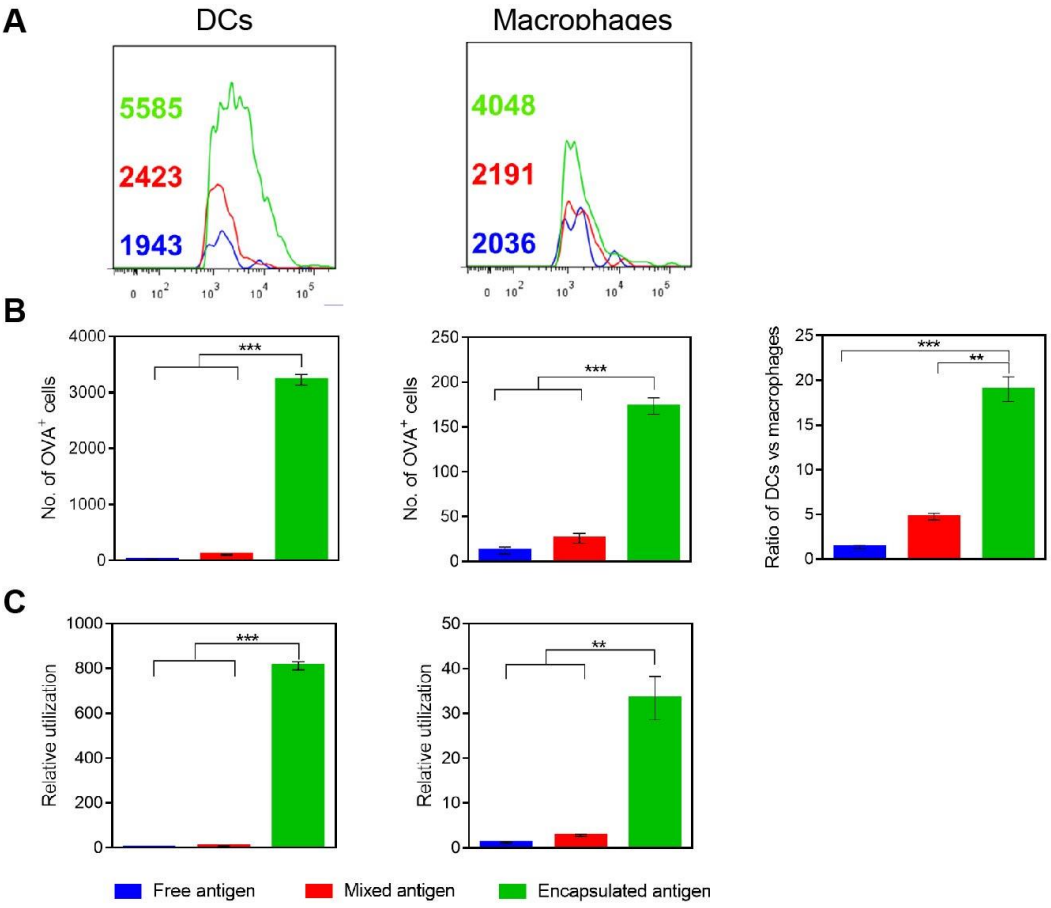

fig. S4. Investigation of OVA internalization by DC and macrophage.

A) **Antigen uptake amount.** Compared with free antigen, mixed antigen moderately improved the antigen uptake amount by DCs rather than macrophages. Once the antigen was encapsulated for vaccination, we achieved further significant improvement for both DCs and macrophages.

B) **Number of OVA$^+$ cell.** Compared with free antigen, moderately increased OVA$^+$ DCs and macrophages were detected in mixed antigen group. The number could be further dramatically elevated by the microencapsulation of antigen. Of note, the ratio OVA$^+$ DCs to OVA$^+$ macrophages was detected up to ~19, indicating the domination of DCs recruited at the vaccination site.

C) **Calculation of antigen utilization.** Microcapsule formulation significantly improved the antigen utilization, especially for DCs. (n=3).

The bars in A-C represented means±s.d..

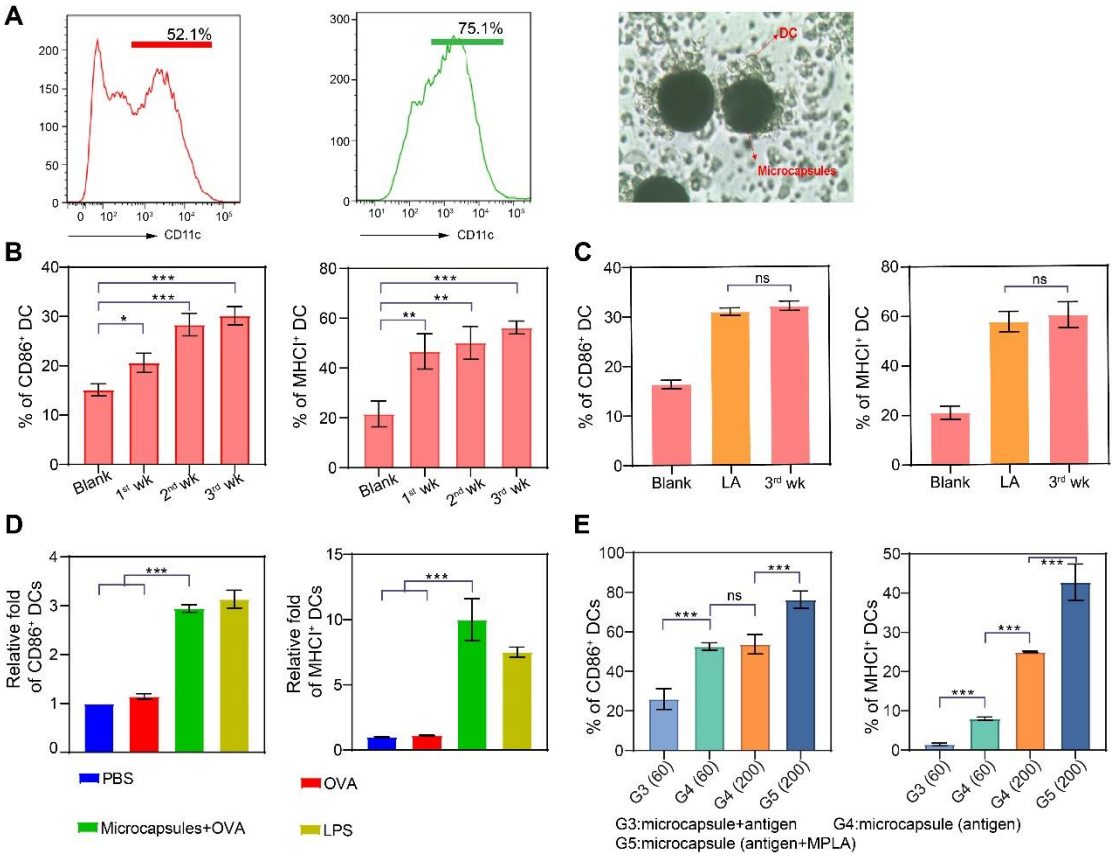

fig. S5. Complementary investigations on primary DCs differentiation, activation and cross-presentation.

A) **Effects of microcapsules on primary DCs differentiation *in vitro*.** Left panel: Expression of CD11c on bone marrow DCs (BMDCs) surface after incubation in complete medium (with GM-CSF and IL-4) without microcapsules. Middle panel: Expression of CD11c on bone marrow DCs (BMDCs) surface after incubation in incomplete medium (without GM-CSF and IL-4) with microcapsules. The increased proportion of $CD11c^+$ (from 52.1% to 75.1%) indicated that microcapsules might do a favor for BMDCs differentiation. Right panel: Optical image of DCs in incomplete medium containing microspheres. DCs grew surrounding the microcapsules with dendritic morphology, again confirming the capacity of microcapsules for DCs differentiation.

B) **CD86 and MHC I expression of primary DCs after 24 h incubation with degradation products.** In detail, the microcapsules were incubated in cell culture medium at 37 ℃. Every week, we collected all supernatant by centrifugation and supplemented same volume of cell culture medium. The supernatant together with antigen was then added into the DCs culture medium for 24 h, and the CD86 and MHC I expression were detected. The addition of supernatant led to up-regulated CD86 and MHCI, indicating the degradation components sourced from the microcapsule had the capacity on the DC activation/cross-presentation. (n=3).

C) **CD86 and MHC I expression of primary DCs after 24 h incubation with lactic acid**. The dose of lactic acid was to the degradation product collected at 3rd week. The level of CD86 and MHCI in lactic acid group was approximate to that

of supernatant, which thus confirmed the vital role of lactic acid (LA) on the DC activation/cross-presentation. (n=3).

D) **Primary DCs stimulation with microcapsule formulation *in vitro*.** Compared with the PBS and OVA groups, the expression levels of MHC-I and the co-stimulatory marker CD86 significantly increased in the microcapsule group, indicating a potent DCs stimulation *in vitro*. (n=3).

E) **Influences of formulation-related factors on primary DCs activation and cross-presentation *in vivo*.** G3 (60), antigen (60 μg) mixed with microcapsules; G4 (60), antigen (60 μg)encapsulated in healed microcapsules; G4 (200), antigen (200 μg)encapsulated in healed microcapsules; G5 (200): antigen (200 μg) encapsulated in healed microcapsules with 3 μg MPLA. Compared to G3 group, G4 group with equal dose (60 μg) could improve the DCs activation (indicated by CD86) and cross-presentation (indicated by MHCI), confirming the need for antigen microencapsulation. Once the dose increased to 200 μg in G4 group, we observed an improvement on the expression of MHC I rather than CD86, mostly owing to the increased antigen uptake. With further addition of MPLA in G5 group, both CD86 and MHC I continued to increase, indicating a further improvement on DCs activation and cross-presentation. (n=3).

The bars in B-E represented means±s.d..

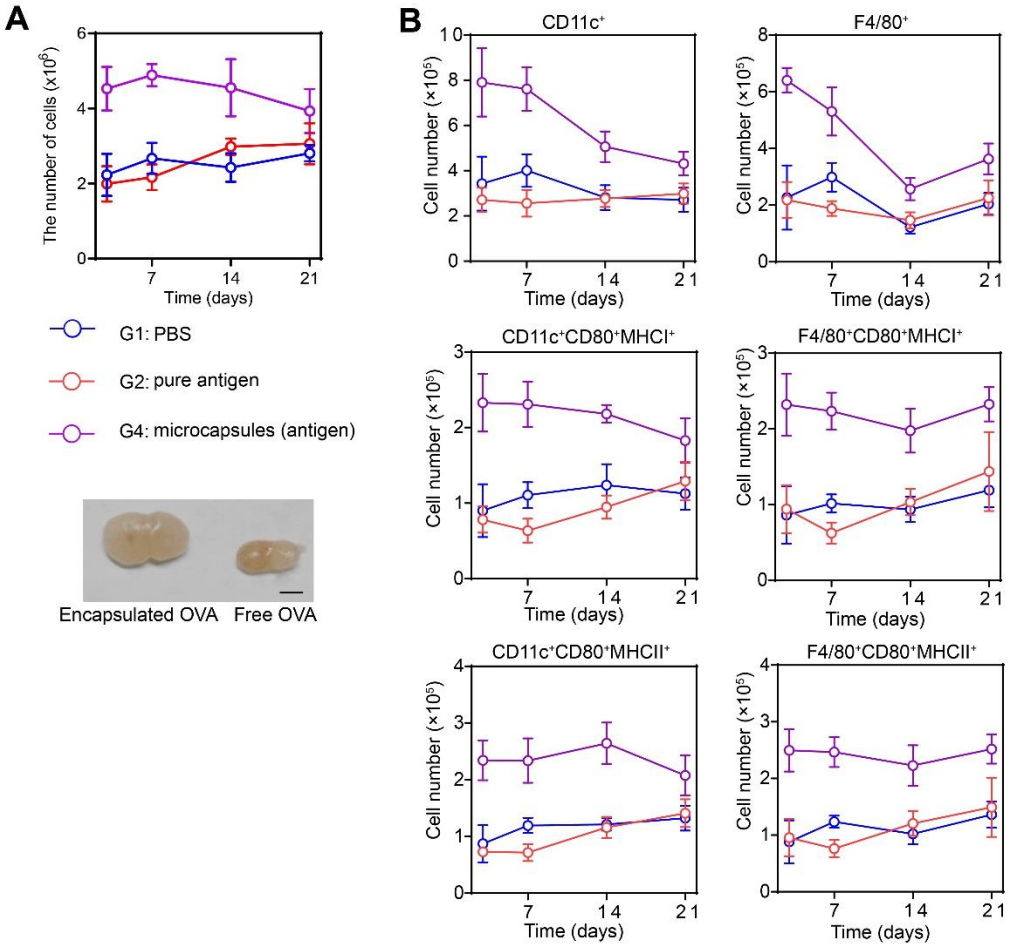

fig. S6. APCs homing to draining lymph nodes (dLNs) and corresponding cellular immune response.

A) **Comparisons of the cells number and size of the dLNs.** G1: PBS; G2: pure antigen (200 μg); G4: antigen encapsulated in microcapsules (200 μg). The cells number of the dLN in encapsulated OVA group increased by ~2-fold compared to that in the free OVA group, and the size of dLN correspondingly increased. Scale bar: 1 mm. (n=3).

B) **The number of DCs and macrophages in dLN after the administration of various vaccines.** Compared to PBS and free OVA groups, the number of DCs and macrophages increased by 4-fold and 3-fold, respectively on day 3 in the encapsulated OVA group. Both activated DCs ($CD11c^+CD80^+MHC\text{-}I^+$, $CD11c^+CD80^+MHC\text{-}II^+$) and macrophages ($F4/80^+CD80^+MHC\text{-}I^+$, $F4/80^+CD80^+MHC\text{-}II^+$) also increased obviously, indicated large amounts of activated APCs homed to dLNs for the subsequent immune response. (n=3).
The bars in A-B represented means±s.d..

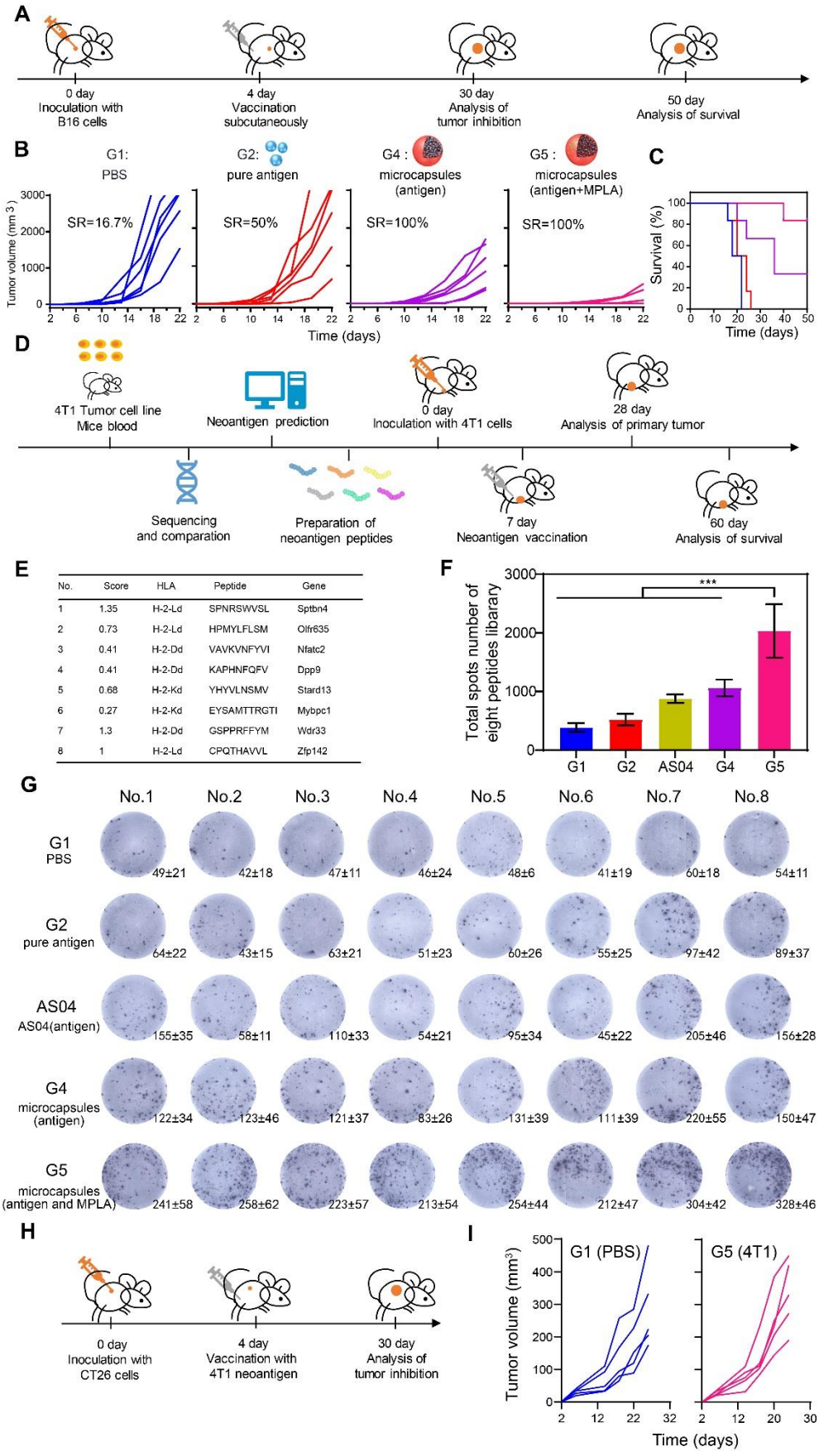
A
0 day
Inoculation with
B16 cells
4 day
Vaccination
subcutaneously
30 day
Analysis of
tumor inhibition
50 day
Analysis of survival
B
G1:
PBS
G2:
pure antigen
G4 :
microcapsules
(antigen)
G5 :
microcapsules
(antigen+MPLA)
SR=16.7%
SR=50%
SR=100%
SR=100%
Tumor volume (mm 3)
Time (days)
C
Survival (%)
Time (days)
D
4T1 Tumor cell line
Mice blood
Neoantigen prediction
0 day
Inoculation with 4T1 cells
28 day
Analysis of primary tumor
Sequencing
and comparation
Preparation of
neoantigen peptides
7 day
Neoantigen vaccination
60 day
Analysis of survival
E
No. Score HLA Peptide Gene
1 1.35 H-2-Ld SPNRSWVSL Sptbn4
2 0.73 H-2-Ld HPMYLFLSM Olfr635
3 0.41 H-2-Dd VAVKVNFYVI Nfatc2
4 0.41 H-2-Dd KAPHNFQFV Dpp9
5 0.68 H-2-Kd YHYVLNSMV Stard13
6 0.27 H-2-Kd EYSAMTTRGTI Mybpc1
7 1.3 H-2-Dd GSPPRFFYM Wdr33
8 1 H-2-Ld CPQTHAVVL Zfp142
F
Total spots number of
eight peptides libarary
***
G1
G2
AS04
G4
G5
G
No.1 No.2 No.3 No.4 No.5 No.6 No.7 No.8
G1
PBS
49±21 42±18 47±11 46±24 48±6 41±19 60±18 54±11
G2
pure antigen
64±22 43±15 63±21 51±23 60±26 55±25 97±42 89±37
AS04
AS04(antigen)
155±35 58±11 110±33 54±21 95±34 45±22 205±46 156±28
G4
microcapsules
(antigen)
122±34 123±46 121±37 83±26 131±39 111±39 220±55 150±47
G5
microcapsules
(antigen and MPLA)
241±58 258±62 223±57 213±54 254±44 212±47 304±42 328±46
H
0 day
Inoculation with
CT26 cells
4 day
Vaccination with
4T1 neoantigen
30 day
Analysis of
tumor inhibition
I
G1 (PBS)
G5 (4T1)
Tumor volume (mm3)
Time (days)

fig. S7. Complementary evaluations of microcapsule vaccine platform in other tumor models.

A) **Scheme of B16-MUC1 tumor inhibition.** The mice were challenged with 5×10^5 B16-MUC1 cells at the axillary and subsequently received single vaccination with different formulations.

B) **B16-MUC1 tumor volume development after different vaccinations.** G1: PBS control; G2: MUC1 peptide (200 μg); G4: MUC1 peptide (200 μg) encapsulated in healed microcapsules; G5: MUC1 peptide (200 μg) encapsulated in healed microcapsules with 3 μg MPLA. Each line represents one animal. Mice were euthanized as their tumor volumes had reached 3000 mm^3. Compared with the unsatisfactory therapeutic effect in the G2 group, the G4 group exhibited a great inhibition on tumor development. With the combination of small dose of MPLA doped (G5), a more potent inhibition could be observed with 3 mice even tumor-free. (n=5).

C) **Survival time of immunized mice in B16-MUC1 bearing mouse model.** A significantly prolonged survival time was observed in G5 group. (n=6).

D) **Scheme of neoantigen production and vaccination in primary tumor.** Detailed description can be seen at the main text and experimental section. G1, PBS control; G2, pure antigen group (200 μg); AS04, antigen (200 μg) mixed with AS04 adjuvant group. G4, antigen (200 μg)encapsulated in healed microcapsules; G5: antigen (200 μg) encapsulated in healed microcapsules with 3 μg MPLA.

E) **Neoantigen peptides used in 4T1 tumor models.** Prediction score, HLA subtype, sequence and corresponding gene of 4T1 neoantigen are listed in the table.

F) **Statistics analysis of IFN-γ ELISpot assays in different groups.** In the aspect of vaccine formulation, the number of total spots increased in the sequence of AS04, microcapsule without MPLA (G4 group) and microcapsule with MPLA (G5 group).

G) **ELISpot analysis of IFN-γ spot-forming cells among splenocytes after *ex vivo* restimulation with neoantigen peptides on day 18.** The mice were administrated with different vaccine formulation at day 7 during the tumor was palpable. All neoantigen peptides used in our manuscript succeeded in induction of immune response, indicating the effectiveness of neoantigen immunotherapy.

H) **Scheme of CT26 tumor inhibition model immunized with 4T1 neoantigen.** The mice were challenged with CT26 cells at the abdomen and subsequently received single vaccination with 4T1 neoantigen-based formulations.

I) **Specificity verification of 4T1 neoantigen peptides in CT26 tumor inhibition model.** G1: PBS treatment. G5 (4T1): vaccination with 4T1 neoantigen peptides. To establish tumor model, CT26 cells (5×10^6) were injected into the abdomen region of the Balb/c mice on day -3. Almost no delay of CT26 tumor development was observed after vaccination with microcapsule vaccine composed of 4T1 tumor neoantigens (G5). On the contrary, the 4T1 tumor development could be well inhibited after same treatment (Fig. 7D). Such a distinct performance thus confirmed the tumor-specificity of the neoantigens. (n=6).

The bars in F represented means±s.d..

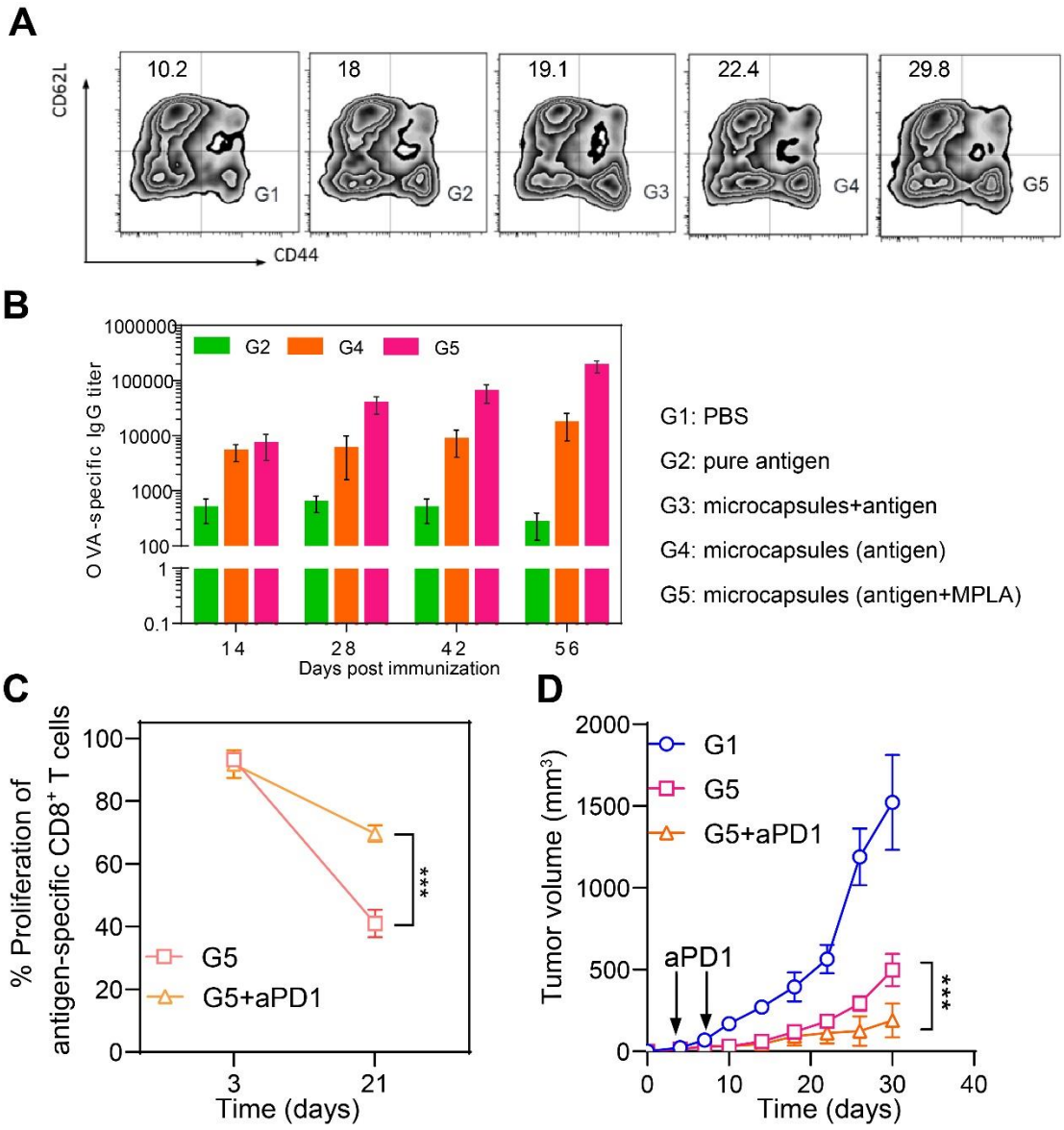

fig. S8. Outlooks about our vaccine platform on prophylactic vaccine and PD-1 antibody combination.

A) **Effect of different vaccination formulations on the memory response.** G1, PBS control; G2, pure antigen group (200 μg); G3, antigen (200 μg) mixed with microcapsules; G4, antigen (200 μg) encapsulated in healed microcapsules; G5: antigen (200 μg) encapsulated in healed microcapsules with 3 μg MPLA. By 28 days after vaccination, the frequency of effector memory T cells (TEM cells, $CD8^+CD44^+CD62L$-) increased to 29.8% in the G5 group, comparing with only 18% in the G2 group. This declared a satisfactory immune memory response aroused by microcapsule vaccine.

B) **ELISA analysis of total OVA-specific IgG response.** Relative to the low-titer antibody response in G3, immunization with the G4 vaccine elicited a strong and durable OVA-specific IgG response, and adjuvant MPLA further enhanced the antibody response (G5). (n=3).

C) **Proliferation of OVA-specific $CD8^+$ T cells at day 3 and 21.** Upon long-term stimulation by tumor vaccine, immune escape always occurred, which typically characterized with PD-1/PD-L1 negative immunoregulatory pathway. PD-1/PD-L1 pathway mainly inhibits immune response by $CD8^+$ T cell dysfunction and apoptosis (T cell exhaustion)/ decreased T cell proliferation/ T-reg phenotype induction. G5 group: microcapsules loading with OVA antigen (200 μg) and MPLA (3 μg); G5+aPD-1 group: G5 vaccination combined with twice intraperitoneal injections of PD-1 antibody (100 μg) at day 4 and day 7. The proliferated antigen specific $CD8^+$ T cell in G5 group dropped to ~40% after 3 weeks, which might be attributed to T cell exhaustion. On the contrary, this could be ameliorated by the PD-1 antibody (aPD-1) combination, and the corresponding value still maintained over 70%. (n=3).

D) **Tumor growth of 4T1 primary tumors after different treatment.** G1 group: PBS control; G5 group: microcapsules (3 mg) loading with 4T1 neoantigen peptides (200 μg) and MPLA (3 μg); G5+aPD-1 group: G5 vaccination combined with twice intraperitoneal injections of PD-1 antibody (100 μg) at day 4 and day 7. At day 30, the tumor volume in G5+aPD-1 group was approximately half of that in G5 group, indicating a step further on the therapeutic outcome against by combination with aPD-1. (n=6).

The bars in B-D represented means±s.d..

Table S1. Analysis of serum biochemical molecules (BUN, ALT, AST, LDH, ALP) at 4th and 8th week after vaccinations. The results were all within the normal range, indicating the long-term safety of the microcapsule vaccine formulations. (n=6).

	BUN	**ALT**	**AST**	**LDH**	**ALP**
G4 (4th week)	9±1	23±5	60±1	920±72	146±5
G4 (8th week)	12±1	33±11	60±10	776±211	133±5
G5 (4th week)	9±1	26±5	53±11	976±40	160±10
G5 (8th week)	12±1	33±5	73±15	653±90	126±15
Normal range	8-33	17-77	54-298	215-1024	60-209